Nature Environment and Pollution Technology
An International Quarterly Scientific Journal

p-ISSN: 0972-6268
(Print copies up to 2016)
e-ISSN: 2395-3454

Vol. 24 | No. 2 | Article ID B4233 | 2025

Original Research Paper

https://doi.org/10.46488/NEPT.2025.v24i02.B4233

Open Access Journal

Delineation of Potential Groundwater Zones Using GIS-based Fuzzy AHP Technique for Urban Expansion in the Southwestern Fringe of Guwahati City, India

Rakesh Kumar Sarmah† and Santanu Sarma
Department of Geology, Cotton University, Guwahati-781001, Assam, India
†Corresponding author: Rakesh Kumar Sarmah; rakeshassam86@gmail.com

Abbreviation: Nat. Env. & Poll. Technol.
Website: www.neptjournal.com

Received: 21-06-2024
Revised: 31-07-2024
Accepted: 07-08-2024

Key Words:

Groundwater potential zones
Groundwater recharge
GIS
Fuzzy AHP
Urban Expansion

Citation for the Paper:

Sarmah, R.K. and Sarma, S., 2025. Delineation of potential groundwater zones using GIS-based fuzzy AHP technique for urban expansion in the southwestern fringe of Guwahati City, India. *Nature Environment and Pollution Technology*, 24(2), p.B4233. https://doi.org/10.46488/NEPT.2025.v24i02.B4233

Note: From year 2025, the journal uses Article ID instead of page numbers in citation of the published articles.

ABSTRACT

Due to unprecedented urban growth many localities within the heart of Guwahati city witness groundwater scarcity, mainly during the dry seasons. This study aims to identify potential groundwater zones in the southwestern fringe of the city where the Guwahati Metropolitan Development Authority (GMDA) has adopted plans for future expansion. Rani and Chayani Barduar are two administrative blocks adjacent to the city, possessing a vast tract of unsettled agricultural land ideal for future township development. Multi-criteria decision-making technique using a Fuzzy Analytical Hierarchy Process (FAHP) in a Remote Sensing and Geographic Information System (GIS) environment is used to produce the groundwater potential map. A total of eight thematic layers important for groundwater recharge: lithology, geomorphology, slope, rainfall, lineament density, soil, drainage density, and Land Use Land Cover are prepared using satellite data, fieldwork, and other suitable techniques and used as input. The study area is classified into five groundwater potential zones – very high (42.52 %), high (28.67 %), moderate (17.23%), poor (10.21 %), and very poor (1.37%). Validation of the result using a yield map derived from the exploratory wells of the Central Ground Water Board (CGWB) shows strong agreement with the prediction accuracy (AUC = 73.36%). Field-derived water level data also show a high negative correlation (R^2 = 0.71) with yield data indicating high specific yield in wells with shallow water levels. The study results will help planners and policymakers with future urban development strategies and sustainable groundwater management practices.

INTRODUCTION

Groundwater is a vital renewable resource that requires proper management to ensure long-term use (Mays 2013). Though groundwater occupies only a small portion (0.06%) of Earth's available water, it is the most critical freshwater source used for drinking purposes (Schwartz & Zhang 2002). The expanding population, unscientific exploitation, and improper management of groundwater in developing countries have led to the deterioration of both quality and quantity and thus demand a critical assessment for sustainable management (Tolche 2021). Groundwater will be the key parameter in achieving many of the Sustainable Development Goals targeted by the United Nations (Guppy et al. 2018). The underground water stock depends on percolation through porous spaces of soils and rocks, which in turn determines urban water supply and agricultural activity (Da Costa et al. 2019). Assessment of groundwater potential zones is important to counteract water scarcity problems caused by various factors such as rapid urbanization, climate change, uneven distribution of water resources, etc. (Raju et al. 2019). In India, about 400 million people live in urban areas, resulting in changes in LULC, including deforestation and an increase in impervious surfaces affecting groundwater recharge and thus causing an acute shortage of water (Roy et al. 2022). Guwahati, the gateway to northeast India, is one of the fastest-growing cities in India. Guwahati had a population of 43,615 (1951 census) and subsequently increased to 9,63,429 in the 2011 census (Desai et al. 2014). It is estimated that Guwahati will house approximately 22 lakh residents by 2025. To tackle this rapidly growing scenario, the Guwahati Metropolitan Development Authority (GMDA) has adopted specific Master Plans for Greater Guwahati with extended spatial periphery to previously untouched rural areas. The greater Guwahati metropolitan area, which presently covers an area of 262 sq. km, is going to cover 328 square kilometers by 2025 (GMA 2025). Topographically the south-western fringe of Guwahati city has vast tracts of unsettled agricultural land and thus is ideal for future expansion. Urbanization will come with different facets, such as industrialization, sprawl, waste management, irrigation, contamination, and their complex interactions. Thus an assessment of the groundwater potential zone is mandatory for the city planners to counteract any future negative consequences. The integrated use of remote sensing and Geographic Information Systems (GIS) in groundwater studies has been well documented in various literature (Nas & Berktay 2008, Moghaddam et al. 2013, Rahmati et al. 2014, Freitas et al. 2019, Sandoval & Tiburan Jr. 2019, Gaurav & Singh 2022, Sabale et al. 2024, Rehman et al. 2024, Ganesan & Subramaniyan, 2024, Sharma et al. 2024), especially due to its time and cost-effectiveness (Kumar et al. 2016). Researchers have adopted different multivariate statistical techniques in estimating groundwater potential; however, the Analytical Hierarchy Process (AHP) is preferred due to its ease of integration with remote sensing and the GIS environment (Celik 2019, Dar et al. 2020, Lentswe & Molwalefhe 2020, Bennia et al. 2023, Hilal et al. 2024). GIS plays a vital role in spatial decision-making, where a large number of alternatives need to be analyzed (Rikalovic et al. 2014). Though the Analytical Hierarchy Process (AHP), developed by Saaty, is one of the most versatile decision-making techniques that has been used to solve complex problems involving competition for multiple choices (Rezaei & Tahsili 2018), there is a chance of vagueness and uncertainty in crisp judgment by human reasoning which can be overcome by introducing fuzziness to the process (Torabi-Kaveh et al. 2016). Fuzzy set theory is a specially designed mathematical tool to deal with such uncertainty, vagueness, and imprecision (Kahraman et al. 2004). It was originally introduced by Lotfi Zadeh in the 1960s with the implementation of classes or groups of data that are not sharply defined & have a blurred boundary resembling closely real-world problems (Brasil et al. 1998).

STUDY AREA

The study area includes the Rani and Chayani Barduar administrative block of Kamrup – Metro (Guwahati city) and the Kamrup-Rural Districts of Assam, covering an area of 423.03 sq. km containing 130 villages. Urbanization is prominent towards the north, adjacent to the Guwahati Airport. Fig. 1 shows a hill shade map of the study area prepared using SRTM DEM. The Brahmaputra River flows north of the study area. Physiography of the area is mainly the

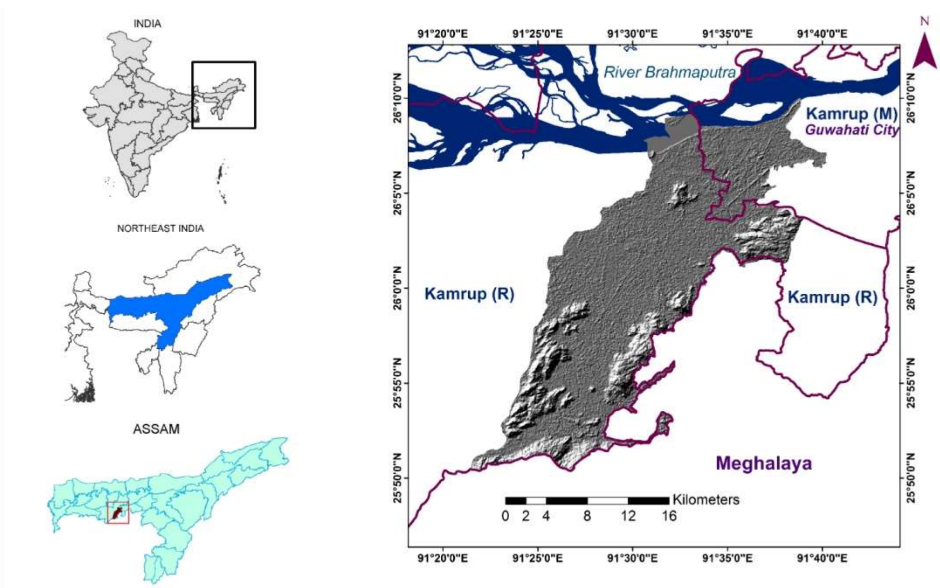

Fig. 1: SRTM DEM derived hill shade map of the area showing Rani and Chayani Barduar administrative blocks located at the southwestern fringe of Guwahati city, Assam, India.

floodplains of the river Brahmaputra and its tributaries, along with hilly terrains and isolated hillocks of the Meghalaya plateau in the south.

The region witnesses a tropical monsoon-type climate, with rainfall occurring between June to September. The average temperature ranges from 35ºC in summer to 9ºC in winter. Though the Brahmaputra River flows adjacent to the study area, significant urban populations traditionally rely on groundwater sources due to the inadequate supply and capacity of water treatment plants. Inequitable distribution, unplanned development of aquifers, gradual reduction in subsurface infiltration due to increased urbanization, and noticeable changes in seasonal rainfall patterns are some factors that led to water scarcity within the city as well as surrounding areas, especially in dry seasons (Das & Goswami 2013). Therefore, an assessment of the groundwater prospect zone is necessary to ensure future urban expansion potential.

MATERIALS AND METHODS

Multiple parameters play a dominant role in groundwater recharge, and these are used to estimate the groundwater potential. The number of thematic layers that can be used also depends on the availability of data for the study region. As per the report by the Central Ground Water Board, the chief source of groundwater recharge in the Himalayan region is the glaciers, and in the foothill region, rainfall plays the dominant role, contributing a copious amount. In Northeast India, groundwater occurrence can be witnessed in weathered residuum and fractures/ joints in consolidated formations in the Assam and Meghalaya plateau, semi-consolidated porous formations of tertiary rocks, and unconsolidated formations of Quaternary age in the Brahmaputra & Barak valleys (Gupta 2014). Based on the literature survey, expert opinion, and in consultation with local hydro-geologists, the following parameters and their relative importance are considered for the estimation of groundwater potential in the study area: lithology, geomorphology, slope, land use land cover, rainfall, soil, lineament density, and drainage density.

Lithology maps are prepared using data from the Bhukosh platform of the Geological Survey of India. For geomorphology maps, the ISRO/ Bhuvan portal is used as a reference. Soil maps are prepared using datasets from the National Bureau of Soil Survey and Land Use Planning, Government of India. Slope and drainage density are prepared using the Digital Elevation Model (DEM) of the Shuttle Radar Topography Mission (SRTM). Lineament density and LULC maps are prepared using Landsat 8 satellite imagery. Rainfall data is collected from the GIOVANNI application of NASA. The groundwater yield map is prepared using data from the Central Groundwater Board (CGWB). Static water table data is collected by field survey. Remote sensing and GIS are mainly used in preparing different layers. Arc GIS 10.7, ERDAS Imagine 10, and ENVI 5.6 are the prime GIS software used for the rectification, digitization, resampling, and processing of various data.

Weight assignment to the parameters and their corresponding classes is carried out using the Fuzzy Analytical Hierarchy Process (FAHP) based on their relative importance to groundwater recharge. Literature surveys of groundwater potential estimation in similar terrains and climatic conditions provide an overview of the contribution of different parameters and insight regarding the assignment of weights. For example, in an AHP-based analysis of groundwater potential estimation by Ahmed & Sajjad (2017) in the lower Barapani watershed, adjacent to the current study area, the pair-wise comparison between lithology and slope is assigned a weight of 5 on Saaty's scale, indicating lithology is fairly important compared to slope for groundwater recharge as lithology is important for the development of slopes. Melese & Belay (2022) conducted a similar analysis in the Abay Basin, Ethiopia, a tropical to subtropical basin with variable topography of plains and hills assigning significant pair-wise weightage to geology, lineament density, drainage density, and rainfall, and relatively less weightage to LULC. Roy et al. (2024) assign the highest pair-wise weightage to rainfall and the lowest to LULC in groundwater potential estimation of the Dooars region of West Bengal, India, a sub-Himalayan foothill region dominated by monsoon precipitation. The study area falls under the primary rainfed zones of the State due to its adjacency to the Shillong plateau, the wettest region of the Earth. Rainfall is the primary contributor to the groundwater reserve and is given more weightage than the other parameters in a pair-wise comparison. Similarly, the lithology and geomorphology of the area are influenced by a broad geological timeframe, from Precambrian elevated hills to recent alluvial deposits by river Brahmaputra and its tributaries influencing the groundwater reserve, which are given the second highest assignment in the comparison matrix followed by the lineament density, which is the surface signatures of the potential groundwater reserve. Due to adequate rainfall and topographic relief, the area is abundant in perennial and seasonal tributaries, facilitating surface runoff and negatively influencing the groundwater regime. The drainage density and soil parameters are assigned with the subsequent pair-wise importance, followed by the LULC with the least assignment, as the same is influenced by other parameters.

A fuzzy set is characterized by a membership function that assigns to each object a grade of membership ranging between zero and one. Mathematically, if *X* is a universal set, a fuzzy set Ă in *X* is characterized by its membership function denoted by $\mu_{\breve{A}}$, so that $\mu_{\breve{A}} : X \rightarrow [0,1]$ (Bhargava 2013). Though there are several different forms of membership functions, triangular and trapezoidal membership functions are extensively used due to their simplicity and efficiency in real-time computation (Azam et al. 2020). In this study, the triangular fuzzy membership function is used for computational ease. Before the implementation of the FAHP method, the Analytical Hierarchy Process (AHP) developed by Saaty is used to check the consistency of the decisions by the decision maker. It uses a pairwise comparison matrix to calculate the weights for each criterion involved (Chakraborty & Joshi 2014). Though the nine-point AHP scale by Saaty gives information about the dominance of each parameter above the other, the fixed value discrete scale judgment cannot simplify the information unpredictability, creating a weak spot in decision-making. However, fuzzy set theory with its interval judgment (Table 1) deals with such impreciseness (Kaganski et al. 2018). The consistency of the comparison matrix is validated using the crisp weight of Saaty's scale (Table 1) and Saaty's standard ratio index (Radulovi´c et al. 2022). The matrix consistency is assessed using the Consistency Index (CI) formula: $CI = \frac{\lambda_{\max} - n}{n-1}$ where $\lambda_{\max}$ is the principal eigenvalue of the pairwise comparison matrix, and n is the number of parameters used in the analysis. The Consistency Ratio (CR) is determined by dividing the Consistency Index (CI) by the Ratio Index (RI). For consistency of the weight, the CR value should be less than 0.1. If CR is higher than 0.1, re-evaluation within the matrix is needed (Tošovic´-Stevanovic' et al. 2020). The CR for this particular study is found to be 0.03, which is in the acceptable range.

Buckley's column geometric mean method is used to get the final normalized weight. The process uses the center-of-area method as the de-fuzzification technique. To obtain the normalized weights of the parameters, first, the defuzzification process is applied to get the crisp values using the arithmetic mean of the fuzzy members (l,m,u), followed by normalizing the weights by dividing each value by the sum of the criteria weight to get the normalized sum of 1 (Ally et al. 2021, Baalousha et al. 2023). The following mathematical equations are used in this study (Bayer & Karamasa 2018).

Table 1: Linguistic scale for FAHP pair-wise comparison (Ayhan 2013).

Saaty Scale	Definition	Fuzzy Triangular Scale
1	Equally important	(1,1,1)
3	Weakly important	(2,3,4)
5	Fairly important	(4,5,6)
7	Strongly important	(6,7,8)
9	Absolutely important	(9,9,9)
2, 4, 6, 8	The intermittent values between two adjacent scales	(1,2,3), (3,4,5), (5,6,7), (7,8,9)

The membership function for triangular fuzzy numbers is defined by the triplet indicating the smallest possible value, the most promising value, and the largest possible value. The membership function is defined by the following equation:

$$\mu_{\widetilde{M}}(x) = \begin{cases} \frac{(x-l)}{(m-l)}, l \leq x \leq m, \\ \frac{(u-x)}{(u-m)}, m \leq x \leq u \\ 0, otherwise \end{cases}$$

A triangular fuzzy number $\widetilde{M}$ is shown in the Fig. 2

Fuzzy pair-wise matrices can be represented as

$$\tilde{B} = \left(\tilde{b}_{ij}\right)_{n\times k}$$

$$\begin{bmatrix} (1,1,1) & (l_{12}, m_{12}, u_{12}) & \ldots & (l_{1k}, m_{1k}, u_{1k}) \\ (l_{21}, m_{21}, u_{21}) & (1,1,1) & \cdots & (l_{2k}, m_{2k}, u_{2k}) \\ \vdots & \vdots & \cdots & \vdots \\ (l_{n1}, m_{n1}, u_{n1}) & (l_{n2}, m_{n2}, u_{n2}) & \cdots & (1,1,1) \end{bmatrix}$$

Where $\tilde{b}_{ij=} \left(l_{ij}, m_{ij}, u_{ij}\right), \tilde{b}_{ij}^{-1} = (\frac{1}{u_{ji}}, \frac{1}{m_{ji}}, \frac{1}{l_{ji}})$

For i = 1,2,3,….n; j = 1,2,3,….,k elements and $i \neq j$

New pair-wise comparison matrix averaging preferences for all decisions:

$$\tilde{B} = \begin{bmatrix} \widetilde{b_{11}} & \widetilde{b_{12}} & \cdots & \widetilde{b_{1n}} \\ \widetilde{b_{21}} & \widetilde{b_{22}} & \cdots & \widetilde{b_{2n}} \\ \cdots & \cdots & \cdots & \cdots \\ \widetilde{b_{m1}} & \widetilde{b_{m2}} & \cdots & \widetilde{b_{mn}} \end{bmatrix}$$

The geometric mean of each criterion is calculated by:

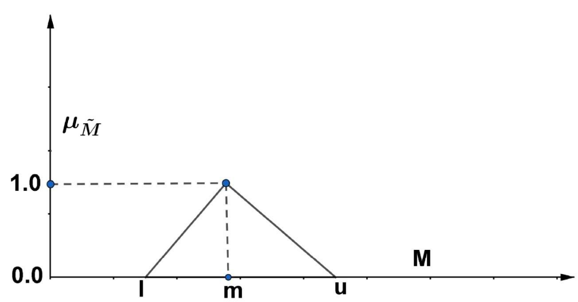

Fig. 2: Graphical representation of a triangular fuzzy membership function.

$$\widetilde{h_\iota} = \left[\prod_{j=1}^{n} \widetilde{b_{\iota J}}\right]^{1/n} \text{ Where, } i = 1,2, \ldots, m$$

Fuzzy weights of each criterion are obtained by:

$$\widetilde{w_1} = \widetilde{h_\iota} \otimes \left(\widetilde{h_\iota} \oplus \widetilde{h_2} \oplus \ldots \oplus \widetilde{h_n}\right)^{-1} = (l_i, m_i, u_i)$$

Centre of area de-fuzzification technique to transform fuzzy weights into crisp ones:

$$k_i = \frac{l_i + m_i + u_i}{3}$$

Crisp weights to normalized final weight:

$$z_i = \frac{k_i}{\sum_{i=1}^{m} k_i}$$

Finally, a weighted linear combination method (Das & Pal 2019, Mallick et al. 2019) is used in the GIS environment to delineate potential groundwater zones.

$$GWPZ = (RF_w \times RF_{wc}) + (LTw \times LT_{wc}) + (GM_w \times GM_{wc}) + (LD_w \times LD_{wc}) + (DD_w \times DD_{wc}) + (S_w \times S_{wc}) + (SL_w \times SL_{wc}) + (LU_w \times LU_{wc})$$

Where, GWPZ = Groundwater Potential Zone, RF = Rainfall, LT = Lithology, GM = Geomorphology, LD = Lineament Density, DD = Drainage Density, S = Soil, SL = Slope, LU = Land Use Land Cover, *w* = Normalized weight of the parameters and *wc* = Normalized weight of the corresponding classes of the parameters.

The methodological flowchart adopted for this study (Fig. 3) illustrates the sequential steps involved, starting from data acquisition (e.g., remote sensing imagery, geological maps) to analytical techniques (e.g., fuzzy logic, GIS-based mapping) and final interpretation. This structured approach ensures a comprehensive evaluation of groundwater recharge zones within the study area.

RESULTS AND DISCUSSION

Lithology

Lithology controls the percolation of water flow, thus influencing groundwater recharge rates (Yeh et al. 2016). Rocks with less compaction, a higher degree of weathering, and fracturing are suitable for groundwater recharge (Senanayake et al. 2016). The dominant geological formations encountered within the study area (Fig. 4a) are alluviums of the Brahmaputra River and its tributaries and Precambrian rocks of the Meghalaya plateau. The alluvial deposits can be categorized into two parts: older alluvium (covering 6.5 % area), consisting of reddish and brownish coarse sand particles with irregularly distributed, unsorted pebbles deposited during Pleistocene, and newer alluvium (53.6 %) consisting of light-colored sand, silt, and clay deposited during recent geological time. These alluvium deposits are ideal for groundwater recharge, providing good porosity and permeability conditions. The Precambrian rocks

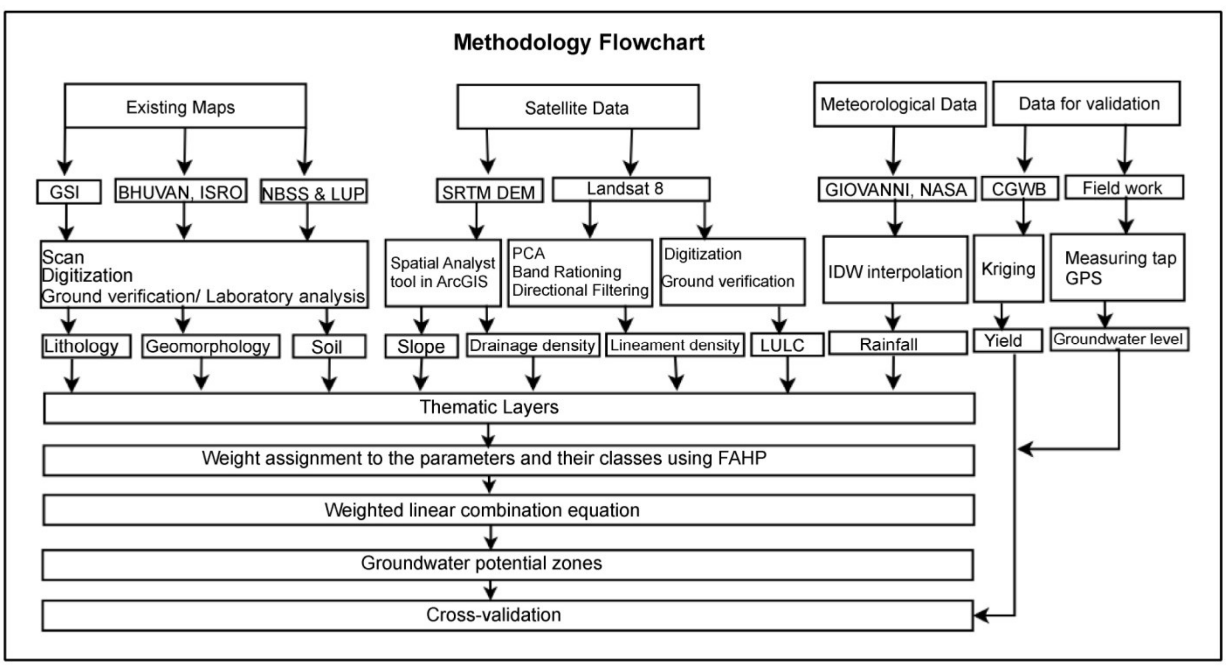

Fig. 3: The methodological flowchart adopted for this study.

Table 2: Fuzzy comparison matrix and normalized weight for different classes of lithology.

Classes	Migmatite, Granitic Gneiss	Older Alluvium	Newer Alluvium	Normalized weight
Migmatite, Granitic Gneiss	1,1,1	1/6, 1/5, 1/4	1/6, 1/5, 1/4	0.10
Older Alluvium	4,5,6	1,1,1	1,1,1	0.45
Newer Alluvium	4,5,6	1,1,1	1,1,1	0.45

(39.8 %) mainly consist of gneisses intruded by pegmatites and quartz. Granitic gneiss is the dominant rock unit of the area, showing a concordant relationship with all other foliated rock units. Hard rock lithology is usually not suitable for groundwater recharge except for significant amounts of weathering and fracturing conditions.

The suitability of different lithological classes for groundwater recharge is quantitatively assessed using a fuzzy comparison matrix. The normalized weights assigned to each lithological class are presented in Table 2.

Geomorphology

In combination with structures and lithology, geomorphic features control the occurrence of groundwater (Solomon & Quiel 2006). The distinguishable geomorphic features within the study area (Fig. 4b) are a) Floodplains: The study area witnesses periodic flooding due to the Brahmaputra river in the north, along with its tributary channels flowing from the Meghalaya plateau in the south. The floodplains contain old meanders, paleochannels, natural levees, back swamps, wetlands, and channel bars. Both active and older floodplains can be identified within the study area. b) Alluvial plains: Alluvial plains within the study area occur at a slightly higher elevation than the floodplains. Both younger and older alluviums can be identified within the area. c) Piedmont zone: The Piedmont zone is mainly concentrated towards the south of the study area at the foothill region consisting of eroded materials of adjacent denudational hills. d) Denudational hills: Relict hills of the Precambrian plateau are mainly formed by stream erosion. These are moderate to highly dissected gneissic hills.

Flood plains and alluvial plains are assigned the highest rank in terms of groundwater recharge, followed by the Piedmont zone and gneissic hills. The normalized weights assigned to each geomorphic class are presented in Table 3.

Slope

The slope of the area (Fig. 4c) directly affects the controlling factors of groundwater availability. A steeper slope results in more runoff than infiltration, causing less chance of groundwater recharge (Rani et al. 2015). The study area is divided into five classes based on slope angle: 0^o-5^o (flat), 5^o-15^o (gentle), 15^o-30^o (moderate), 30^o-45^o (steep), and 45^o-89^o (very steep) (Fig. 4c). 70.86 % and 14.72 % of the study areas fall under the “flat” and “gentle” category, indicating promising groundwater reserves. The fuzzy comparison matrix and the corresponding normalized weight for each slope class are presented in Table 4.

Land Use Land Cover (LULC)

Land use land cover patterns and changes significantly affect groundwater quality and quantity (Singh et al. 2010, He et al. 2019). LULC of the study area (Fig. 4d) is delineated using Landsat 8 satellite imagery using ArcGIS 10.7 software based on visual image interpretation technique, followed by field verification. Major LULC classes include agricultural land/

Table 3: Fuzzy comparison matrix and normalized weight for different classes of geomorphology.

Class	Denudational Hills	Pediment Pediplain Complex	Alluvial Plain/Flood Plain	Water bodies	Normalized weight
Denudational Hills	1, 1, 1	1/3, 1/2, 1	1/4, 1/3, 1/2	1/6, 1/5, 1/4	0.10
Pediment Pediplain Complex	1, 2, 3	1, 1, 1	1/3, 1/2, 1	1/4, 1/3, 1/2	0.14
Alluvial Plain/ Flood Plain	2, 3, 4	1, 2, 3	1, 1, 1	1/3, 1/2, 1	0.24
Water bodies	4, 5, 6	2, 3, 4	1, 2, 3	1, 1, 1	0.52

Table 4: Fuzzy comparison matrix and normalized weight for different classes of slope.

Slope	45^o-89^o (very steep)	30^o-45^o (steep)	15^o-30^o (moderate)	5^o-15^o (gentle)	0^o-5^o (flat)	Normalized weight
45^o-89^o (very steep)	1, 1, 1	1/3, 1/2, 1	1/4, 1/3, 1/2	1/6, 1/5, 1/4	1/7, 1/6, 1/5	0.04
30^o-45^o (steep)	1, 2, 3	1, 1, 1	1/3, 1/2, 1	1/4, 1/3, 1/2	1/6, 1/5, 1/4	0.06
15^o-30^o (moderate)	2, 3, 4	1, 2, 3	1, 1, 1	1/3, 1/2, 1	1/4, 1/3, 1/2	0.10
5^o-15^o (gentle)	4, 5, 6	2, 3, 4	1, 2, 3	1, 1, 1	1/3, 1/2, 1	0.22
0^o-5^o (flat)	5, 6, 7	4, 5, 6	2, 3, 4	1, 2, 3	1, 1, 1	0.58

Table 5: Fuzzy comparison matrix and normalized weight for different classes of LULC.

LULC	Built-up	Forest	Agricultural Land/ Grassland/ Wasteland	Water bodies	Normalized weight
Built-up	1, 1, 1	1/4, 1/3, 1/2	1/5, 1/4, 1/3	1/6, 1/5, 1/4	0.06
Forest	2, 3, 4	1, 1, 1	1/4, 1/3, ½	1/5, 1/4, 1/3	0.10
Agricultural Land/ Grassland/ Wasteland	3, 4, 5	2, 3, 4	1, 1, 1	1/4, 1/3, 1/2	0.21
Water bodies	4, 5, 6	3, 4, 5	2, 3, 4	1, 1, 1	0.63

household plantation (54.91%) and forest cover (27.16%). Both classes are given a higher weight because they can hold a substantially high proportion of water (Agarwal et al. 2013, Arulbalaji et al. 2019). The fuzzy comparison matrix and normalized weight for different LULC classes are presented in Table 5.

Rainfall

The Tropical Rainfall Measuring Mission version 7 product (TRMM V7) was used for rainfall estimation over the study area for ten years (2010-2019). TRMM V7, available in GIOVANNI (Geospatial Interactive Online Visualization and Analysis Infrastructure), is a web-based application developed by NASA. It outperforms other remote sensing precipitation products as it contains real-time gridded precipitation (3B42RTV7) with near-global coverage along with gauge-adjusted post-real-time research product (3B42V7) having high spatial (0.25°) and temporal (3 hours) resolution (Liu et al. 2016). The average annual rainfall map is prepared using the IDW interpolation technique, taking 10 years of rainfall over the study area (Fig. 4e). The fuzzy comparison matrix and normalized weight for different classes of rainfall are presented in Table 6.

Lineament Density

Lineaments are subsurface expressions in topography associated with faults - linear fracturing and bending deformation that indicate increased permeability of the crust (Florinsky 2016). Faults and fracture zones play important roles in groundwater dynamics and are indicators of feeding for the aquifer (Ammar & Kamal 2018). Landsat 8 satellite with Operational Land Imager (OLI) captured bands are used to delineate lineaments by adopting various digital image enhancement techniques. Out of different techniques, Principal Component Analysis (PCA), band rationing, and directional filtering are commonly used for extracting the lineaments of the study area (Fig. 4f). PCA analysis carried out using band 1 to band 7 gives principal components, and PC (1, 2, 3) reveals structural information (Mathew & Ariffin 2018).RGB composite of band ratios (7/5, 6/4, 4/2) is suitable for enhancing lithological features (Al-Nahmi et al. 2016). Directional convolution filtering is applied on band 6 of Landsat 8 imagery using ENVI software in four directions N-S (0^o), NE-SW (45^o), E–W (90^o), and NW–SE (135^o), highlighting the main lineament directions of the study area (Javhar et al. 2019). The fuzzy comparison matrix and

Table 6: Fuzzy comparison matrix and normalized weight for different classes of rainfall.

Classes	3163.00 – 3380.50 mm	3380.50 – 3598.03 mm	3598.03 – 3815.60 mm	3815.60 – 4033.06 mm	4033.06 – 4250.58 mm	Normalized Weight
3163.00 – 3380.50 mm	1, 1, 1	1/3, 1/2, 1	1/4, 1/3, 1/2	1/5, 1/4, 1/3	1/6, 1/5, 1/4	0.07
3380.50 – 3598.03 mm	1, 2, 3	1, 1, 1	1/3, 1/2, 1	1/4, 1/3, 1/2	1/5, 1/4, 1/3	0.13
3598.03 – 3815.60 mm	2, 3, 4	1, 2, 3	1, 1, 1	1/3, 1/2, 1	1/5, 1/4, 1/3	0.20
3815.60 – 4033.06 mm	3, 4, 5	2, 3, 4	1, 2, 3	1, 1, 1	1/3, 1/2, 1	0.27
4033.06 – 4250.58 mm	4, 5, 6	3, 4, 5	2, 3, 4	1, 2, 3	1, 1, 1	0.33

Table 7: Fuzzy comparison matrix and normalized weight for different classes of lineament density.

Lineament Density	0 – 0.29	0.29 – 0.58	0.58 – 0.87	0.87 – 1.17	1.17 – 1.46	Normalized weight
0 – 0.29	1, 1, 1	1/3, 1/2, 1	1/4, 1/3, 1/2	1/5, 1/4, 1/3	1/6, 1/5, 1/4	0.07
0.29 – 0.58	1, 2, 3	1, 1, 1	1/3, 1/2, 1	1/4, 1/3, 1/2	1/5, 1/4, 1/3	0.13
0.58 – 0.87	2, 3, 4	1, 2, 3	1, 1, 1	1/3, 1/2, 1	1/5, 1/4, 1/3	0.20
0.87 – 1.17	3, 4, 5	2, 3, 4	1, 2, 3	1, 1, 1	1/3, 1/2, 1	0.27
1.17 – 1.46	4, 5, 6	3, 4, 5	2, 3, 4	1, 2, 3	1, 1, 1	0.33

normalized weight for different LULC classes of lineament density are presented in Table 7.

Soil

Groundwater recharge and quality are influenced by the spatial variation of soil types (Rukundo & Dogan 2019). A Soil map of the area (Fig. 4g) is prepared using a soil classification scheme developed by the National Bureau of Soil Survey & Land Use Planning (NBSS&LUP). Soil samples were collected and analyzed in the laboratory to determine soil parameters, mainly for texture and drainage conditions. The data are plotted in a GIS environment, and the 'natural neighbor' interpolation technique is adopted to show the distribution of soil types. Fine-grained soils facilitate less infiltration due to less permeability in comparison to coarse-grained soil. Therefore, a lower rank is given for soils with a fine-grained texture and a higher rank for soils with a coarse-grained texture. The fuzzy comparison matrix and normalized weight for different classes of soil are presented in Table 8.

Drainage Density

Drainage density is a measure of the total stream length to the total basin area (Strahler 1964) and is often expressed in $km.km^{-2}$. Lower drainage density indicates higher permeability, with greater infiltration of rainfall resulting in good groundwater conditions (Magesh et al. 2012). The drainage network of the study area is extracted from SRTM DEM (30 m spatial resolution) using the Hydrology tool under the Spatial Analyst Toolbox of ArcGIS 10.7. The drainage density is calculated using the line density tool (Fig. 4h). The fuzzy comparison matrix and normalized weight for different classes of drainage density are presented in Table 9.

Table 10 shows the Fuzzy comparison matrix and normalized weight for all the controlling parameters.

Delineation of Groundwater Potential Zonation

The groundwater potential zones were classified into five categories based on the *GWPZ* equation – Very High (179.87 km^2, 42.52%), High (121.28 km^2, 28.67%), Moderate (72.89 km^2, 17.23 %), Poor (43.19 km^2, 10.21%) and Very Poor (5.80 km^2, 1.37%) (Fig. 5a). Very high and high groundwater potential areas are found mainly in low-lying flat/gentle flood plains and alluvial plains towards the north of the study area. Towards the south, eroded hills with high lineament density are also having high groundwater potential. Proximity to the river Brahmaputra, the presence of wetlands, vast areas of unsettled agricultural land, as well as basin-like topography due to the surrounding elevated landforms of the Shillong plateau is some justification against this abundance of groundwater. Moderate groundwater potential areas are mainly found toward the south of the study area; it comprises the piedmont pediplain complex and hills having moderate lineament density. Poor and very poor groundwater potential areas are found in steeper gneissic hills with relatively moderate to low rainfall and low lineament density. These areas fall under the reserve forest, and human settlement is not authorized.

The study results have been compared with findings by other researchers adopting similar approaches in different

Table 8: Fuzzy comparison matrix and normalized weight for different classes of soil.

Soil	Typic Dystrochrepts (Clayey Fine loamy)	Umbric Dystrochrepts (Fine loamy skeletal)/ Fluventic Dystrochrept (Fine loamy	Aeric Haplaquepts (Fine silty	Aeric Fluvaquent (coarse silty)	Normalized weight
Typic Dystrochrepts (Clayey Fine loamy)	1, 1, 1	1/3, 1/2, 1	1/4, 1/3, ½	1/4, 1/3, ½	0.11
Umbric Dystrochrepts (Fine loamy skeletal)/Fluventic Dystrochrept (Fine loamy	1, 2, 3	1, 1, 1	1/3, 1/2, 1	1/4, 1/3, 1/2	0.15
Aeric Haplaquepts (Fine silty	2, 3, 4	1, 2, 3	1, 1, 1	1/3, 1/2, 1	0.30
Aeric Fluvaquent (coarse silty)	2, 3, 4	2, 3, 4	1, 2, 3	1, 1, 1	0.44

Table 9: Fuzzy comparison matrix and normalized weight for different classes of drainage density.

Drainage Density	2.67 - 3.34	2.00 - 2.67	1.33 - 2.00	0.66 - 1.33	0 - 0.66	Normalized weight
2.67-3.34	1, 1, 1	1/3, 1/2, 1	1/4, 1/3, 1/2	1/5, 1/4, 1/3	1/6, 1/5, 1/4	0.07
2.00-2.67	1, 2, 3	1, 1, 1	1/3, 1/2, 1	1/4, 1/3, 1/2	1/5, 1/4, 1/3	0.13
1.33-2.00	2, 3, 4	1, 2, 3	1, 1, 1	1/3, 1/2, 1	1/5, 1/4, 1/3	0.20
0.66-1.33	3, 4, 5	2, 3, 4	1, 2, 3	1, 1, 1	1/3, 1/2, 1	0.27
0-0.66	4, 5, 6	3, 4, 5	2, 3, 4	1, 2, 3	1, 1, 1	0.33

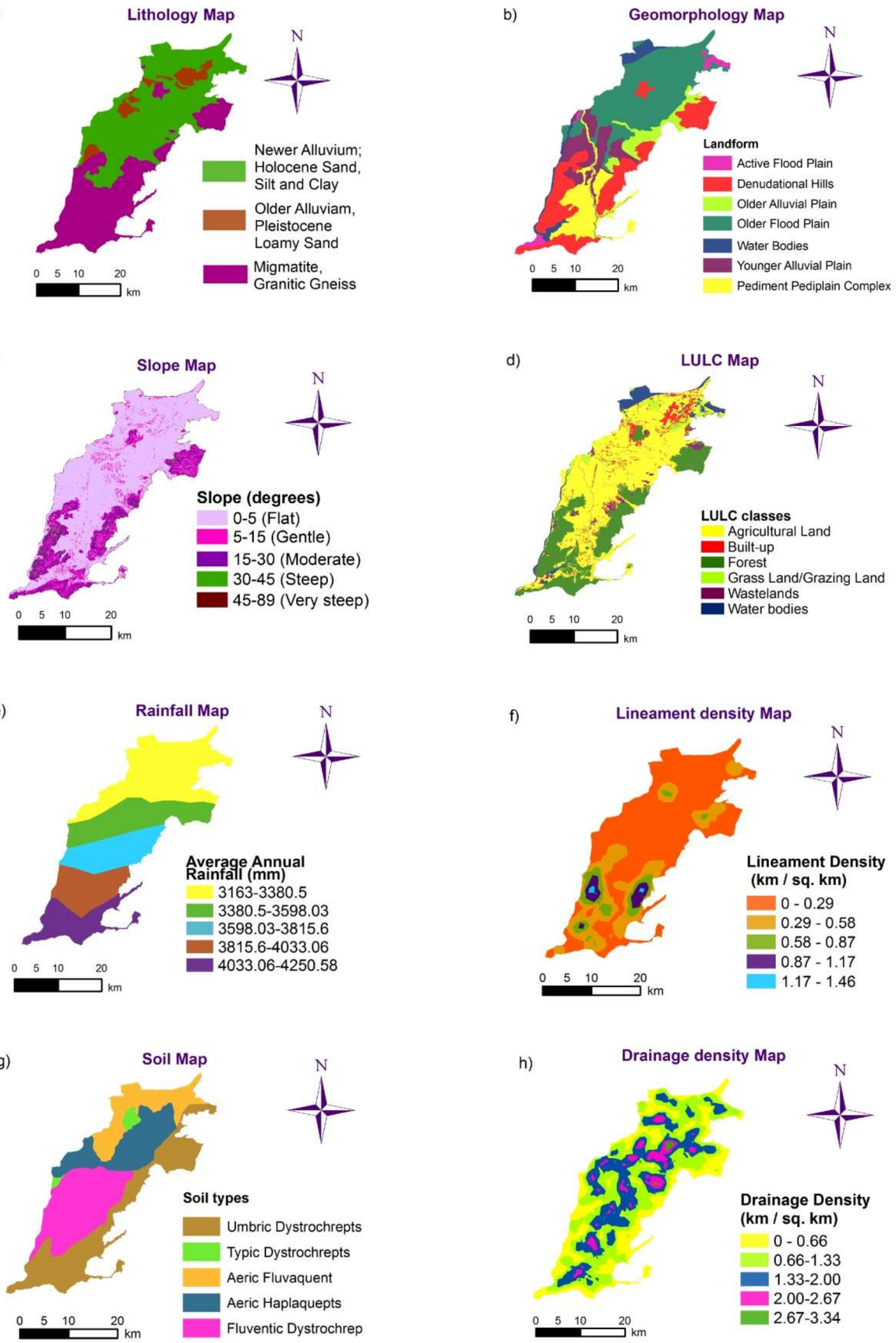

Fig. 4: Thematic layers important for groundwater recharge a) Lithology, b) Geomorphology, c) Slope, d) LULC, e) Rainfall, f) Lineament density, g) Soil, and h) Drainage density.

Table 10: Fuzzy comparison matrix and normalized weight for controlling parameters.

Parameters	Rainfall	Lithology	Geomorphology	Lineament Density	Drainage Density	Soil	Slope	LULC	Normalized Weights
Rainfall	1, 1, 1	1, 2, 3	1, 2, 3	2, 3, 4	2, 3, 4	4, 5, 6	5, 6, 7	6, 7, 8	0.27
Lithology	1/3, 1/2, 1	1, 1, 1	1, 2, 3	1, 2, 3	2, 3, 4	3, 4, 5	4, 5, 6	5, 6, 7	0.18
Geomorphology	1/3, 1/2, 1	1/3, 1/2, 1	1, 1, 1	1, 2, 3	2, 3, 4	3, 4, 5	4, 5, 6	5, 6, 7	0.18
Lineament Density	1/4, 1/3, 1/2	1/3, 1/2, 1	1/3, 1/2, 1	1, 1, 1	1, 2, 3	2, 3, 4	5, 6, 7	5, 6, 7	0.14
Drainage Density	1/4, 1/3, 1/2	1/4, 1/3, 1/2	1/4, 1/3, 1/2	1/3, 1/2, 1	1, 1, 1	1, 2, 3	2, 3, 4	3, 4, 5	0.09
Soil	1/6, 1/5, 1/4	1/5, 1/3, 1/3	1/5, 1/3, 1/3	1/4, 1/3, 1/2	1/3, 1/2, 1	1, 1, 1	2, 3, 4	2, 3, 4	0.09
Slope	1/7, 1/6, 1/5	1/6, 1/5, 1/4	1/6, 1/5, 1/4	1/7, 1/6, 1/5	1/4, 1/3, 1/2	1/4, 1/3, 1/2	1, 1, 1	1, 2, 3	0.03
LULC	1/8, 1/7, 1/6	1/7, 1/6, 1/5	1/7, 1/6, 1/5	1/7, 1/6, 1/5	1/7, 1/6, 1/5	1/5, 1/3, 1/3	1/4, 1/3, 1/2	1/3, 1/2, 1	0.03

terrains to understand the commonalities involved. For example, the AHP-based groundwater potential estimation in the Kashmir Valley by Dar et al. (2020) revealed identical results with excellent groundwater potential in the alluvial plains of the basin deposited by river Jhelum and its tributaries and poor to very poor potential in the mountainous

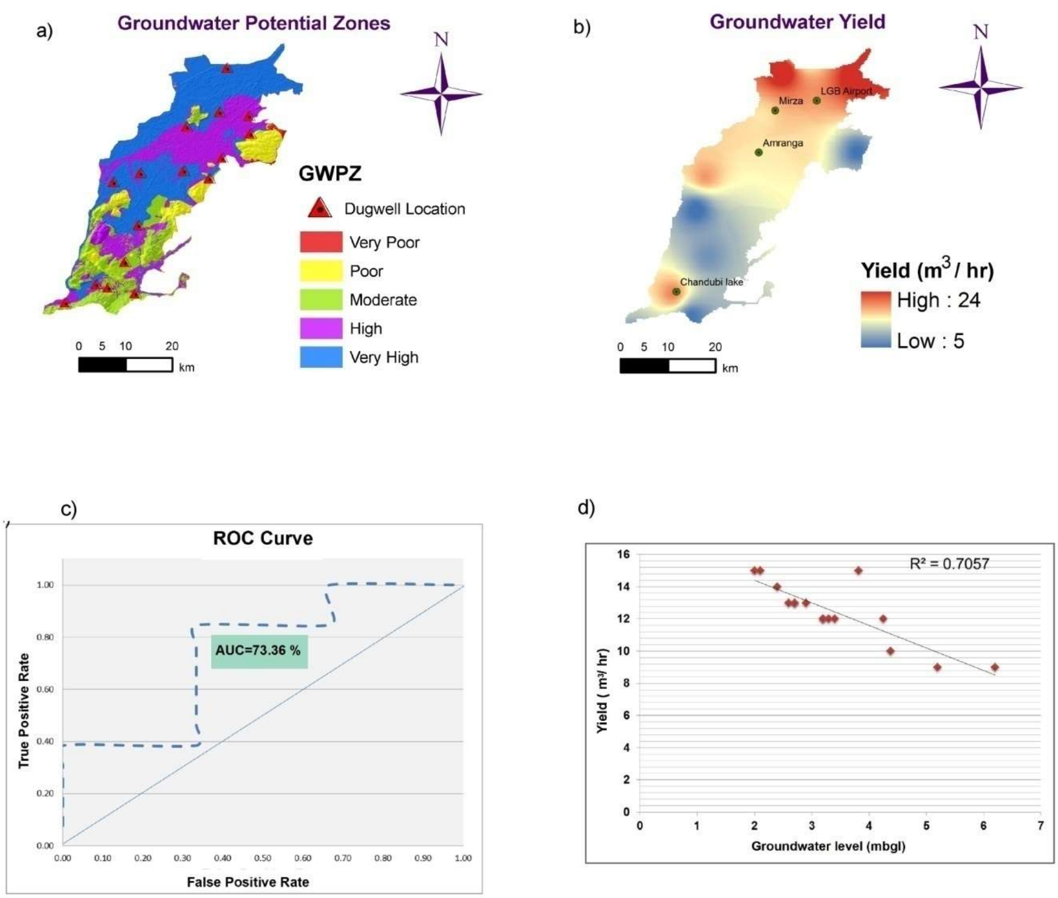

Fig. 5 a: Groundwater potential zone map, b) Groundwater yield map prepared using CGWB data, c) Receiver Operating Characteristic (ROC) curve for validation, d) Relationship between groundwater yield and mean annual groundwater level.

areas, denudational hills with steeper slopes with high runoff and less infiltration. GIS-based fuzzy AHP analysis by Bhadran et al. (2022) also shows very good aquifer potential in the coastal areas of Karuvannur River Basin, Kerala, with a high alluvial cover and poor groundwater prospects in the eastern periphery of the basin with hard rock lithology. Radulovi´c et al. (2022) found similar results with good to very good groundwater potential zones in the alluvial plains of the Danube and Tisa Rivers and very poor and poor potential zones in the loess plateau due to high runoff and poor water retention capacity. Aouragh et al. (2017), in a fuzzy GIS-based analysis of the Middle Atlas plateaus, Morocco, observed promising groundwater zones in areas with concentrated limestone fractures.

Validation

The zones are validated by generating a yield map (Fig. 5b) using yield data of exploratory wells drilled by the Central Ground Water Board (CGWB) and field-derived static water table data of household dug wells. The highest yield of 24 $m^3.h^{-1}$ is observed in low-lying flood plains areas, and the lowest yield of 5 $m^3 \cdot h^{-1}$ is observed in gneissic hills, showing an agreement with FAHP-derived groundwater potential zonation. Quantitative validation of the Receiver Operating Characteristic (ROC) curve (Fig. 5c) analysis shows the Area Under the Curve (AUC) to be 73.36%, indicating good prediction accuracy of the method (Kumar & Krishna 2016, Andualem & Demeke 2019). Fieldwork was conducted in 16 households dug wells in both pre and post-monsoon and the mean annual groundwater level was measured. Before the field visit for groundwater level collection, the area is divided into a 5km × 5km grid using ArcGIS software to collect samples at regular intervals. Groundwater level (mbgL) shows a negative correlation with yield data with an R^2 value of 0.71, indicating high specific yield in wells with shallow water levels and vice versa (Fig. 5d).

CONCLUSIONS

Remote Sensing and GIS-based groundwater potential zone delineation using the FAHP technique are efficient as well as cost-effective. Satellite remote sensing coupled with limited field verification and laboratory work can assist in preparing a database of selected parameters influencing groundwater recharge, such as rainfall, lithology, geomorphology, lineament density, drainage density, soil, slope, and land use land cover. GIS allows the analysis of various parameters under a single platform. Different parameters have different degrees of influence in groundwater recharge, and their relative importance needs to be assessed for decision-making. The Fuzzy Analytical Hierarchy Process (FAHP) is feasible in prioritizing one parameter above the other by assigning weights in a pairwise comparison manner considering the real-world subjective judgments. Similarly, different classes under each parameter are allocated weights, and a potential groundwater map is prepared in the GIS environment. Very high and high groundwater potential areas are found towards the north in low-lying flat flood plains and alluvial plains; moderate potential areas are piedmont pediplain complex and hills having moderate lineament density, poor and very poor potential areas are steeper gneissic hills having relatively moderate to low rainfall and low lineament density. Validation of the groundwater potential map with yield map and field-derived water level data gives satisfactory agreement with the obtained result. The study area lies towards the southwest of Guwahati city and has the potential for future urban expansion. As the city witnesses water scarcity due to the rapid growth of population and infrastructure, a prior assessment is needed in its fringe areas for sustainable urban expansion. This type of pilot study is helpful in decision-making processes for the professionals and policymakers involved in groundwater, urban planning, and allied sectors.

ACKNOWLEDGMENTS

The authors would like to thank different government and nongovernment organizations for providing valuable data, and various regional experts for their valuable suggestions and guidance. The authors give special thanks to Mr. Thatey Mohamed Zuhail for his valuable guidance regarding manuscript preparation.

REFERENCES

Agarwal, E., Agarwal, R., Garg, R.D. and Garg, P.K., 2013. Delineation of groundwater potential zone: an AHP/ANP approach. *Journal of Earth System Science*, 122, pp. 887-898. [DOI]

Ahmed, R. and Sajjad, H., 2018. Analyzing factors of groundwater potential and its relation with population in the lower Barapani watershed, Assam, India. *Natural Resources Research*, 27, pp. 503-515. [DOI]

Ally, A.M., Yan, J., Bennett, G., Lyimo, N.N. and Mayunga, S.D., 2024. Assessment of groundwater potential zones using remote sensing and GIS-based fuzzy analytical hierarchy process (F-AHP) in Mpwapwa District, Dodoma, Tanzania. *Geosystems and Geoenvironment*, 3, p.100232. [DOI]

Al-Nahmi, F., Alami, O.B., Baidder, L., Khanbari, K., Rhinane, H. and Hilali, A., 2016. Using remote sensing for lineament extraction in Al Maghrabah area - Hajjah, Yemen. *The International Archives of the Photogrammetry, Remote Sensing and Spatial Information Sciences*, XLII-2/W1, pp. 137-142. [DOI]

Ammar, A.I. and Kamal, K.A., 2018. Resistivity method contribution in determining fault zone. *Applied Water Science*, 8, pp.1-27. [DOI]

Andualem, T.G. and Demeke, G.G., 2019. Groundwater potential assessment using GIS and remote sensing: A case study of Gunatana landscape, upper Blue Nile Basin, Ethiopia. *Journal of Hydrology: Regional Studies*, 24, p.100610. [DOI]

Aouragh, M.H., Essahlaoui, A., El Ouali, A., El Hmaidi, A. and Kamel, S., 2017. Groundwater potential of Middle Atlas plateaus, Morocco, using the fuzzy logic approach, GIS, and remote sensing. *Geomatics, Natural Hazards and Risk*, 8(2), pp.194-206. [DOI]

Arulbalaji, P., Padmalal, D. and Sreelash, K., 2019. GIS and AHP techniques based delineation of groundwater potential zones: a case study from Southern Western Ghats, India. *Scientific Reports*, 9, p.2082. [DOI]

Ayhan, M.B., 2013. A fuzzy AHP approach for supplier selection problem: a case study in a gearmotor company. *International Journal of Managing Value and Supply Chains*, 4(3), pp.11-23. [DOI]

Azam, M.H., Hasan, M.H., Hassan, S. and Abdulkadir, S.J., 2020. Fuzzy type-1 triangular membership function approximation using fuzzy C-means. In: B. S. Iskandar (ed.) *International Conference on Computational Intelligence (ICCI)*. IEEE, Manhattan, NY, USA, pp.64-78.

Baalousha, H.M., Younes, A., Yassin, M.A. and Fahs, M., 2023. Comparison of the fuzzy analytic hierarchy process (F-AHP) and fuzzy logic for flood exposure risk assessment in arid regions. *Hydrology*, 10, p.136. [DOI]

Bayer, R.U. and Karamasa, C., 2018. Analyzing destination attributes under fuzzy environment: a case study in Eskişehir. *European Journal of Tourism Research*, 18, pp.75-94. [DOI]

Bennia, A., Zeroual, I., Talhi, A. and Kebir, W., 2023. Groundwater potential mapping using the integration of AHP method, GIS and remote sensing: a case study of the Tabelbala region, Algeria. *Bulletin of the Mineral Research and Exploration*, 172, pp.41-60. [DOI]

Bhadran, A., Girishbai, D., Jesiya, N.P., Gopinath, G., Krishnan, R.G. and Vijesh, V.K., 2022. A GIS-based fuzzy-AHP for delineating groundwater potential zones in a tropical river basin in the southern part of India. *Geosystems and Geoenvironment*, 1, p.100093. [DOI]

Bhargava, A.K., 2013. *Fuzzy Set Theory Fuzzy Logic and their Applications*. S. Chand, pp.18-19.

Brasil, L.M., Mendes de Azevedo, F., Barreto, J.M. and Noirhomme-Fraiture, M., 1998. Complexity and cognitive computing. In: J. Mira, A.P. and M. Ali (eds.) *Methodology and Tools in Knowledge-Based Systems*. IEA/AIE 1998, *Lecture Notes in Computer Science*, Springer, Berlin, Heidelberg, pp.145-163.

Celik, R., 2019. Evaluation of groundwater potential by GIS-based multicriteria decision making as a spatial prediction tool: A case study in the Tigris River Batman-Hasankeyf sub-basin. *Water*, 11(12), pp.1-16. [DOI]

Chakraborty, A. and Joshi, P.K., 2014. Mapping disaster vulnerability in India using analytical hierarchy process. *Geomatics, Natural Hazards and Risk*, 7(1), pp.308-325. [DOI]

Da Costa, A.M., De Salis, H.H.C., Viana, J.H.M. and Pacheco, F.A.L., 2019. Groundwater recharge potential for sustainable water use in urban areas of the Jequitiba River basin. *Sustainability*, 11(10), pp.1-20. [DOI]

Dar, T., Rai, N. and Bhat, A., 2020. Delineation of potential groundwater recharge zones using analytical hierarchy process (AHP). *Geology, Ecology, and Landscapes*, 5(4), pp.292-307. [DOI]

Das, B. and Pal, S.C., 2019. Combination of GIS and fuzzy-AHP for delineating groundwater recharge potential zones in the critical Goghat-II block of West Bengal, India. *HydroResearch*, 2, pp.21-30. [DOI]

Das, N. and Goswami, D.C., 2013. A geo-environmental analysis of the groundwater resource vis-a-vis surface water scenario in Guwahati city. *Current World Environment*, 8(2), pp.275-282. [DOI]

Desai, R., Mahadevia, D. and Mishra, A., 2014. *City Profile: Guwahati*. Centre for Urban Equity (CUE). Retrieved June 13, 2020, from Link

Florinsky, I.V., 2016. *Digital Terrain Analysis in Soil Science and Geology*. Elsevier, Academic Press, p.13.

Freitas, L., Afonso, M.J., Pereira, A.J.S.C., Delerue-Matos, C. and Chamine, H.I., 2019. Assessment of the sustainability of groundwater in urban areas (Porto, NW Portugal): a GIS mapping approach to evaluate vulnerability, infiltration and recharge. *Environmental Earth Sciences*, 78, p.140. [DOI]

Ganesan, S. and Subramaniyan, A., 2024. Identification of groundwater potential zones using multiinfluencing factor method, GIS, and remote sensing techniques in the hard rock terrain of Madurai district, southern India. *Sustainable Water Resources Management*, 10, p.54. [DOI]

Gaurav, N. and Singh, G., 2022. Delineation of groundwater, drought and flood potential zone using weighted index overlay analysis and GIS for District Patna, Bihar, India. *Nature Environment and Pollution Technology*, 21(2), pp.813-828. [DOI]

Guppy, L., Uyttendaele, P., Villholth, K.G. and Smakhtin, V., 2018. *Groundwater and Sustainable Development Goals: Analysis of Interlinkages*. In UNU-INWEH report series. Retrieved June 21, 2020, from Link

Gupta, S., 2014. *Ground Water Scenario of Himalayan Region, India*. Central Ground Water Board. Retrieved November 20, 2020, from Link

Guwahati Metropolitan Development Authority (GMA), 2009. Part 1 Master Plan for Guwahati Metropolitan Area-2025. Retrieved October 17, 2020, from Report.

He, S., Li, P., Wu, J., Elumalai, V. and Adimalla, N., 2019. Groundwater quality under land use/land cover changes: A temporal study from 2005 to 2015 in Xi'an, Northwest China. *Human and Ecological Risk Assessment: An International Journal*, 26(10), pp.2771-2797. [DOI]

Hilal, I., Qurtobi, M., Saadi, R., Aqnouy, M., Bouizrou, I., Bouadila, A., Dakak, H., Abdelrahman, K., MorenoNavarro, J.G., Abioui, M., El Messari, J.E.S., Bessa, A.Z.E. and Benmansour, M., 2024. Integrating remote sensing, GISbased, and AHP techniques to delineate groundwater potential zones in the Moulouya Basin, NorthEast Morocco. *Applied Water Science*, 14, p.122. [DOI]

Javhar, A., Chen, X., Bao, A., Jamshed, A., Yunus, M., Jovid, A. and Latipa, T., 2019. Comparison of multi-resolution optical Landsat-8, Sentinel-2 and radar Sentinel-1 data for automatic lineament extraction: a case study of Alichur area, SE Pamir. *Remote Sensing*, 11(7), p.778. [DOI]

Kaganski, S., Majak, J. and Karjust, K., 2018. Fuzzy AHP as a tool for prioritization of key performance indicators. *Procedia CIRP*, 72, pp.1227-1232. [DOI]

Kahraman, C., Cebeci, U. and Ruan, D., 2004. Multi-attribute comparison of catering service companies using fuzzy AHP: The case of Turkey. *International Journal of Production Economics*, 87(2), pp.171-184. [DOI]

Kumar, A. and Krishna, A.P., 2016. Assessment of groundwater potential zones in coal mining impacted hard-rock terrain of India by integrating geospatial and analytic hierarchy process (AHP) approach. *Geocarto International*, 33(2), pp.105-129. [DOI]

Kumar, P., Herath, S., Avtar, R. and Takeuchi, K., 2016. Mapping of groundwater potential zones in Killinochi area, Sri Lanka, using GIS and remote sensing techniques. *Sustainable Water Resources Management*, 2, pp.419-430. [DOI]

Lentswe, G.B. and Molwalefhe, L., 2020. Delineation of potential groundwater recharge zones using analytic hierarchy process-guided GIS in the semi-arid Motloutse watershed, eastern Botswana. *Journal of Hydrology: Regional Studies*, 28, pp.1-22. [DOI]

Liu, S., Yan, D., Qin, T., Weng, B. and Li, M., 2016. Correction of TRMM 3B42V7 based on linear regression models over China. *Advances in Meteorology*, 16, pp.1-13. [DOI]

Magesh, N.S., Chandrasekar, N. and Soundranayagam, J.P., 2012. Delineation of groundwater potential zones in Theni district, Tamil Nadu, using remote sensing, GIS, and MIF techniques. *Geoscience Frontiers*, 3(2), pp.189-196. [DOI]

Mallick, J., Khan, R.A., Ahmed, M., Alqadhi, S.D., Alsubih, M., Falqi, I. and Hasan, M.A., 2019. Modeling groundwater potential zone in a semi-arid region of Aseer using fuzzy-AHP and geoinformation techniques. *Water*, 11(12), p.2656. [DOI]

Mathew, T.G. and Ariffin, K.S., 2018. Remote sensing technique for lineament extraction in association with mineralization pattern in central belt peninsular Malaysia. In: M. Jaafar and K.A. Razak (eds.) *Journal of Physics: Conference Series*, 14, pp.12-29. [DOI]

Mays, L.W., 2013. Groundwater resources sustainability: Past, present, and future. *Water Resources Management*, 27, pp.4409–4424. [DOI]

Melese, T. and Belay, T., 2022. Groundwater potential zone mapping using analytical hierarchy process and GIS in Muga Watershed, Abay Basin, Ethiopia. *Global Challenges*, 6, p.2100068. [DOI]

Moghaddam, D.D., Rezaei, M., Pourghasemi, H.R., Pourtaghie, Z.S. and Pradhan, B., 2013. Groundwater spring potential mapping using a bivariate statistical model and GIS in the Taleghan watershed, Iran. *Arabian Journal of Geosciences*, 8, pp.913–929. [DOI]

Nas, B. and Berktay, A., 2008. Groundwater quality mapping in urban groundwater using GIS. *Environmental Monitoring and Assessment*, 160, pp.215-227. [DOI]

Rahmati, O., Samani, A.N., Mahdavi, M., Pourghasemi, H.R. and Zeinivand, H., 2014. Groundwater potential mapping at Kurdistan region of Iran using analytic hierarchy process and GIS. *Arabian Journal of Geosciences*, 8, pp.7059–7071. [DOI]

Radulović, M., Brdar, S., Mesaroš, M., Lukić, T., Savić, S., Basarin, B., Crnojević, V. and Pavić, D., 2022. Assessment of groundwater potential zones using GIS and fuzzy AHP techniques—a case study of the Titel municipality (Northern Serbia). *International Journal of Geo-Information*, 11, p.257. [DOI]

Raju, R.S., Raju, G.S. and Rajasekhar, M., 2019. Identification of groundwater potential zones in the Mandavi River basin, Andhra Pradesh, India, using remote sensing, GIS, and MIF techniques. *HydroResearch*, 2, pp.1-11. [DOI]

Rani, V.R., Pandalai, H.S., Sajinkumar, K.S. and Pradeepkumar, A.P., 2015. Geomorphology and its implication in urban groundwater environment: a case study from Mumbai, India. *Applied Water Science*, 5, pp.137-151. [DOI]

Rehman, A., Islam, F., Tariq, A., Ul Islam, I., Brian J, D., Bibi, T., Ahmad, W., Waseem, L.A., Karuppannan, S. and Al-Ahmadi, S., 2024. Groundwater potential zone mapping using GIS and remote sensing-based models for sustainable groundwater management. *Geocarto International*, 39(1), pp.1-27. [DOI]

Rezaei, A. and Tahsili., 2018. Urban vulnerability assessment using AHP. *Advances in Civil Engineering*, 18, pp.1-20. [DOI]

Rikalovic, A., Cosic, I. and Lazarevic, D., 2014. GIS-based multi-criteria analysis for industrial site selection. *Procedia Engineering*, 69, pp. 1054-1063. [DOI]

Roy, D., Barman, S., Mandal, G., Mitra, R., Sarkar, A., Hossain, G., Roy, P., Almohamad, H., Addo, H.G. and Mandal, D.K., 2024. Extracting of prospective groundwater potential zones using remote sensing data, GIS, and multicriteria decisionmaking approach in the SubHimalayan Dooars region of West Bengal, India. *Applied Water Science*, 14, p.72. [DOI]

Roy, S.S., Rahman, A., Ahmed, S., Shahfahad and Ahmed, I.A., 2022. Long-term trends of groundwater level variations in response to local level land use land cover changes in Mumbai, India. *Groundwater for Sustainable Development*, 18, pp.1-10. [DOI]

Rukundo, E. and Dogan, A., 2019. Dominant influencing factors of groundwater recharge spatial patterns in Ergene river catchment, Turkey. *Water*, 11(4), p.653. [DOI]

Sabale, R.S., Babade, S.S., Venkatesh, B. and Jose, M.K., 2024. Application of Arc-SWAT model for water budgeting and water resource planning at the Yeralwadi catchment of Khatav, India. *Nature Environment and Pollution Technology*, 23(1), pp.203-213. [DOI]

Sandoval, J.A. and Tiburan Jr., C.L., 2019. Identification of potential artificial groundwater recharge sites in Mount Makiling forest reserve, Philippines, using GIS and analytical hierarchy process. *Applied Geography*, 105, pp.73-85. [DOI]

Schwartz, F.W. and Zhang, H. 2002. *Fundamentals of Groundwater*. John Wiley & Sons Inc., p.1.

Senanayake, I.P., Dissanayake, D.M.D.O.K., Mayadunna, B.B. and Weerasekera, W.L., 2016. An approach to delineate groundwater recharge potential sites in Ambalantota, Sri Lanka, using GIS techniques. *Geoscience Frontiers*, 7(1), pp.115-124. [DOI]

Sharma, Y., Ahmed, R., Saha, T.K., Bhuyan, N., Kumari, G., Roshani, Pal, S. and Sajjad, H., 2024. Assessment of groundwater potential and determination of influencing factors using remote sensing and machine learning algorithms: a study of Nainital district of Uttarakhand state, India. *Groundwater for Sustainable Development*, 25, p.101094. [DOI]

Singh, S.K., Singh, C.K. and Mukherjee, S., 2010. Impact of land-use and land-cover change on groundwater quality in the Lower Shiwalik hills: a remote sensing and GIS-based approach. *Central European Journal of Geosciences*, 2(2), pp.124-131. [DOI]

Solomon, S. and Quiel, F., 2006. Groundwater study using remote sensing and geographic information systems (GIS) in the central highlands of Eritrea. *Hydrogeology Journal*, 14, pp.1029-1041. [DOI]

Strahler, A.N., 1964. Quantitative geomorphology of drainage basins and channel networks. In: V.T. Chow (ed.) *Handbook of Applied Hydrology*. McGraw-Hill, New York, pp.98-126.

Tolche, A.D., 2021. Groundwater potential mapping using geospatial techniques: a case study of Dhungeta-Ramis sub-basin. *Geology, Ecology, and Landscapes*, 5(1), pp.65-80. [DOI]

Torabi-Kaveh, M., Babazadeh, R., Mohammadi, S. and Zaresefat, M., 2016. Landfill site selection using a combination of GIS and fuzzy AHP, a case study: Iranshahr, Iran. *Waste Management & Research: The Journal for a Sustainable Circular Economy*, 34(5), pp.438–448. [DOI]

Tošović-Stevanović, A., Ristanović, V., Ćalović, D., Lalić, G., Žuža, M. and Cvijanović, G., 2020. Small farm business analysis using the AHP model for efficient assessment of distribution channels. *Sustainability*, 12(24), p.10479. [DOI]

Yeh, H.F., Cheng, Y.S., Lin, H.I. and Lee, C.H., 2016. Mapping groundwater recharge potential zone using a GIS approach in Hualian River, Taiwan. *Sustainable Environment Research*, 26(1), pp.33-43. [DOI]